Journal of Innovative Optical Health Sciences
Vol. 4, No. 2 (2011) 143−150

DOI: 10.1142/S1793545811001368

OPTICALLY TRACKING THE MOTION OF MICROBEADS TO STUDY PHYSICAL BEHAVIORS OF THE LIVING CELL IN RESPONSE TO TRANSIENT STRETCH OR COMPRESSION

LINHONG DENG*, XUEMEI JIANG,
CHENG CHEN, AIJING SONG and FENG LIN
Key Laboratory of Biorheological Science and Technology
Ministry of Education, Chongqing University, Chongqing 400044, China
**denglh@cqu.edu.cn*

Optical magnetic twisting cytometry and traction force microscopy are two advanced cell mechanics research tools that employ optical methods to track the motion of microbeads that are either bound to the surface or embedded in the substrate underneath the cell. The former measures rheological properties of the cell such as cell stiffness, and the latter measures cell traction force dynamics. Here we describe the principles of these two cell mechanics research tools and an example of using them to study physical behaviors of the living cell in response to transient stretch or compression. We demonstrate that, when subjected to a stretch−unstretch manipulation, both the stiffness and traction force of adherent cells promptly reduced, and then gradually recover up to the level prior to the stretch. Immunofluorescent staining and Western blotting results indicate that the actin cytoskeleton of the cells underwent a corresponding disruption and reassembly process almost in step with the changes of cell mechanics. Interestingly, when subjected to compression, the cells did not show such particular behaviors. Taken together, we conclude that adherent cells are very sensitive to the transient stretch but not transient compression, and the stretch-induced cell response is due to the dynamics of actin polymerization.

Keywords: Optical tracking; magnetic twisting; microbeads; motion; stiffness; traction force; cell mechanics.

1. Introduction

In living organisms, many types of adherent cells are subjected to transient stretch. For example, airway smooth muscle cells are transiently stretched during a deep inspiration. Compared to chronic repetitive stretch, transit stretch has been less studied in the past probably due to the difficulty to apply such maneuver to the cell and then measure the corresponding mechanical responses. However, during the last decade, increasing new technologies have emerged, which enable us to tackle more complex problems in cell mechanics. Among these are two optically-based microscopic techniques, namely optical magnetic twisting cytometry (OMTC) and traction force microscopy (TFM).[1,2] Both OMTC and TFM use optical methods to track motion of microbeads that are either bound to the surface of, or embedded in the substrate underneath the cell. With OMTC, the rheological properties of the cell such as cell stiffness can be measured, while with TFM the dynamics of traction force that the cell exerts to its surrounding environment can be quantified. Initially, OMTC and TFM were two separately developed techniques for probing either cell stiffness or intracellular contractile tension. But it was quickly found that, the cell stiffness

quantified by OMTC and the intracellular tension quantified by TFM are actually two closely associated mechanical properties of the cell.[3] Thus, OMTC and TFM become widely used in combination for cell mechanics studies. Furthermore, OMTC and TFM can be supplemented by immunofluorescent staining and confocal microscopy to assess dynamics of the actin cytoskeleton while the cell is subjected to mechanical loading. Together, this suite of optically-based cell assays provides powerful means to investigate the nature of dynamic changes of cellular structure and function in response to mechanical stimulus. The purpose of this article is to introduce to a wider research community the application of these techniques to address important cell mechanics questions and the potential implications to better understanding regulatory mechanisms of health and disease. We first describe the principles of OMTC and TFM, respectively, and then follow with an example of using these techniques to demonstrate that a transient stretch would cause the living cell to fluidize, and upon cessation of the stretch, the cell would gradually resolidify over time.[4–6] In contrast, a transient compression on the cell causes little changes in cell stiffness, suggesting that different mechanisms may be involved in the cell's response to different type of mechanical loading. Examination of the dynamics of the actin cytoskeleton reveals that, the transient stretch-induced cell fluidization may at least, in part, be attributed to the disruption of actin filaments, possibly involving down-regulation of actin binding proteins such as cofilin. All together, it shows that optically tracking the motion of microbeads either on or around the cell can provide useful information regarding cell dynamics, but the observed physical behaviors of the cell in response to transient stretch or compression are far from being fully understood.

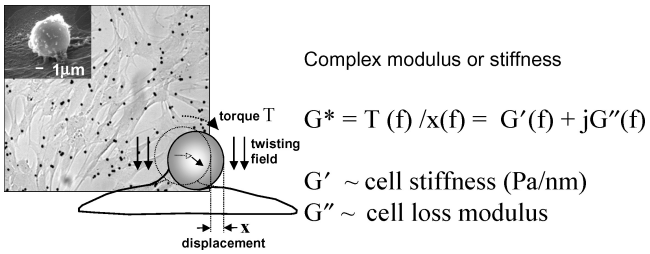

Fig. 1. A sketch presentation of the principle of optical magnetic twisting cytometry — modified from Fabry *et al.* PRL, 2001.[1]

2. Methods and Materials

2.1. *OMTC for measuring cell stiffness*

To measure rheological properties of the cell, particularly the cell stiffness, ferrimagnetic beads (diameter 4.5 μm) were coated with synthetic RGD peptide that would enable the beads to bind specifically to the actin cytoskeleton of the cell via cross-membrane integrin proteins. The GD-coated beads were added to cells cultured in cell culture dishes and allowed to bind to the integrin receptors on the cell surface for about 20 min (as shown in the top left of Fig. 1). Then the beads were magnetized horizontally and subsequently twisted in an oscillatory magnetic field with a frequency of 0.75 Hz (Fig. 2 lower right). The motion of these beads was observed under optical microscope and tracked by consecutive imaging and an algorithm that exacts the bead center position.[1]

The ratio of the applied mechanical torque to the resulting lateral bead displacement was defined as the complex elastic modulus

$$G^* = G' + jG''$$

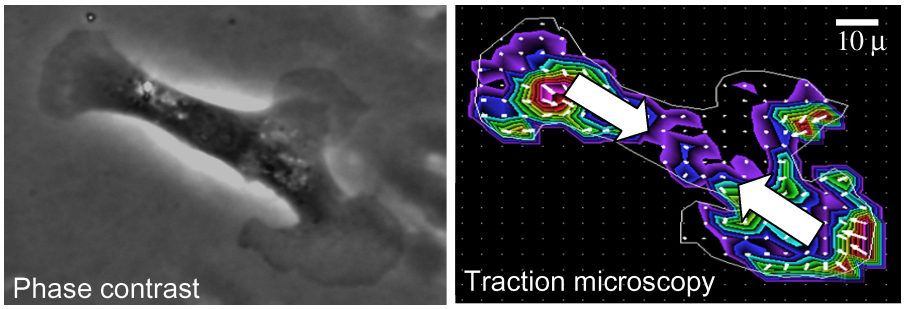

Fig. 2. Phase-contrast image of the cell (left) and fluorescent image of the microbeads embedded in the soft polyacrylamide gel substrate, as well as the computed traction force distribution as shown by the small arrows and the net contractile moment represented by big arrows (right).

where G' is the elastic modulus, or cell stiffness, which has units of Pascal per nanometer, G'' is a loss modulus, and j is the unit imaginary number -1.

2.2. *TFM for measuring cell traction force to the substrate*

To measure the amount of traction force exerted by the cell to its substrate, fluorescent microbeads (diameter 200 nm) were embedded within the soft polyacrylamide gel substrate onto which cells were adhered. The substrate surface was pre-coated with collagen I to promote cell attachment, and the fluorescent microbeads-embedded polyacrylamide gel was prepared according to a previously described protocol.[2,7] Phase-contrast images of the single cell (Fig. 2 left) and images of the fluorescent microbeads directly underneath the cell (Fig. 2 right) were taken at different time points including that during the no-load baseline period, before the onset of the stretch, after stretch cessation, and following cell detachment by trypsinization at the end of experiment. Cell traction field was computed using Fourier transform traction cytometry, which will be described in more detail in the Refs. 7 and 8.

Briefly, the two images of the micropatterned beads plus the phase-contrast cell image were taken to calculate the displacement field of the gel generated by the cell, and the projected cell area was also calculated based on the cell contour determined from the phase-contrast image obtained at the start of the experiment. The image taken after the cell was released from its adhesions by trypsin, i.e., when the gel was free of cell traction force, was used as the reference image, and the displacement field between the reference image and the other image taken at a time when the adherent cell was present was determined by image correlation method (ICM). According to correlation theorem, the Fourier transform of a correlation of two functions, here the two images, is the product of the Fourier transform of one function and the complex conjugate, thus the cross-correlation between the two images can be established and calculated using fast Fourier transform in MATLAB (MathWorks). From this calculation, the coordinates of the peak of the correlation function between these two images can be identified, and one of the images was translated with respect to the other by uniform displacement. Next, the displacement field between the two corrected images is calculated starting from a low spatial resolution and refining the calculation to higher resolutions. Images are first divided into large distinct windows of equal size. The displacement of each window is calculated as described above for the whole images. The procedure is repeated until all the windows in the two images best match each other, which results in a displacement field between these two images. From the displacement field, the traction force that is defined as the stress imposed on the gel substrate by the adherent cell, can be calculated based on the Boussinesq solution for the displacement field on a surface of a semi-infinite solid.[7] For each traction field within a 50 μm $\times$ 50 μm square, the magnitude and the direction of the vectors corresponding to the traction imposed on the gel underneath the cell yielded a scalar measure of cell contractility (net contractile moment, or strain energy), which is the total energy (in pJ) transferred from the cell to the substratum as shown in right panel of Fig. 2.[8]

2.3. *Application of transient biaxial stretch to the cell*

In order to apply a uniform biaxial stretch to the cell, two different devices can be employed. One is a vacuum-driven device that is similar to the conventional Flexcell stretcher but specifically designed to operate under an inverted optical microscope.[4] The other is an annular punch indenter that was designed to deform an elastic substrate under the microscope as shown in Fig. 3(a).[5] The difference between these two methods is that the former applies a stretch to the whole area of the device, whereas the latter can stretch only a portion of the area that is inside the indenter annulus while the area outside the indenter annulus can be kept unstretched. Because of this advantage of the annular punch indenter, we describe it in more detail in the following.

The indenter was mounted to a microscope and set coaxial to the objective lens. When the indenter was lowered manually by a calibrated distance onto the underlying elastic substrate, the surface within the indenter annulus would bulge and thus undergo a stretch (Fig. 3(a), side view). In the central region of this bulged substrate, the imposed strain was nearly uniform and biaxial. The strain was predetermined by the extent of lowering of the indenter.

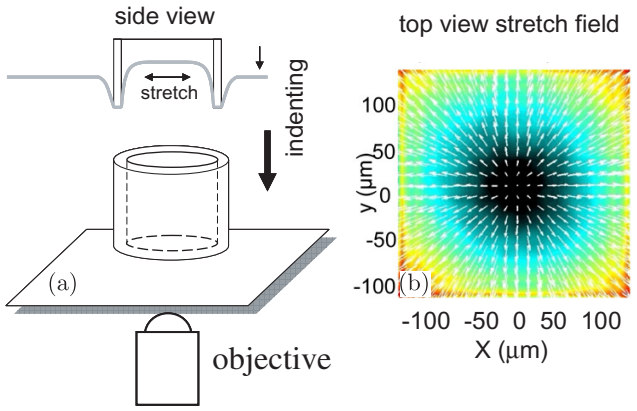

Fig. 3. Sketch of the annular punch indenter for biaxial cell stretch and the side view of stretch profile (a), and the stretch field was verified by the localized vector displacements of fluorescent beads embedded in the substrate gel as indicated by arrows, and their magnitude by color (b) — modified from Krishnan *et al.* PLoS One, 2009.[5]

Accordingly, the cell adherent upon that surface was subjected to a biaxial stretch. When the punch indenter was lifted, the elastic substrate would recoil back to an unstretched state and the cell would have undergone one cycle of transient stretch. This was called a stretch−unstretch maneuver.

The magnitude of the applied biaxial stretch was scalable within the physiological range (0−20%) and highly reproducible. To verify and calibrate the stretch field, fluorescent beads were embedded in the substrate of soft polyacrylamide gel (thickness = 700 μm), and the bead marker positions were obtained before and after a prescribed indentation with the annular punch indenter, in this case with an inner and outer diameter of 2 and 3 mm, respectively. The displacement field was calculated based on relative changes in embedded fluorescent bead marker positions. Despite variable maximal displacement magnitude, the strain field in the central region ($200\,\mu m^2 \times 200\,\mu m^2$) was always almost homogeneous and uniform as shown in Fig. 1.[5]

The experimental protocol of transient stretch−unstretch maneuver to the cell is shown in Fig. 4. For each experiment, the cell was first measured for its baseline values. Then, a 10% stretch was applied to the cell by the punch indenter. The stretch−unstretch maneuver lasted about 4 s. After cessation of the stretch, the measurement was immediately resumed as quickly as possible (in ∼1 s) and repeated at subsequent time points until 300 s.

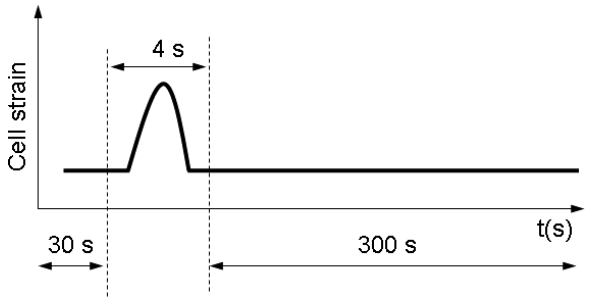

Fig. 4. Experimental protocol of cell stretch. Measurements were first carried out before applying stretch. Then a 10% stretch was quickly applied and released by the punch indenter within 4 s. Measurements were carried out immediately following cessation of the stretch in ∼1 s, and at subsequent time points until 300 s.

2.4. *Cell culture and pharmacological interventions*

Human bladder smooth muscle (HBSM) cells were cultured in Dulbecco's modification of Eagle's medium (DMEM) supplemented with 10% fetal bovine serum (FBS), penicillin (100 U/ml) and streptomycin (100 mg/ml), and were placed in a humidified incubator at 37°C and 5% CO_2. Cells between passages 3−7 were used for all experiments, and they were serum deprived for 24 h before being tested. For OMTC measurements and actin staining, cells were seeded at, 200×10^3 cells/well on gel substrates on deformable membranes (type I collagen coated; Flexcell International Corporation) 24 h before experiment. For traction force measurement, cells were seeded sparsely ($\sim 2 \times 10^3$ cells/well) on type I collagen coated polyacrylamide gel substrates 4 h before experiment; LY294002 (inhibits the PI3K, 10 mM), Triciribine (specifically inhibits the Akt/PKB, 10 mM), SB203580 (inhibits p38 MAP kinase pathway, 10 mM) were used as pharmacological intervention to modulate the cell cytoskeleton.

2.5. *Soft substrate preparation*

Polyacrylamide gel substrates were prepared according to previous protocols.[2,7] The gels were made within 35 mm dishes (glass bottom, uncoated, P35-G-020-C; MaTek). The diameter and the depth of the gel substrates were 20 mm and 700 μm, respectively. The ratio between acrylamide (Bio-Rad Laboratory) and bis-acrylamide (Bio-Rad Laboratory) were adjusted to be 40 and 2%, respectively,

resulting in a Young's modulus at 4 kPa that is optimal for cell proliferation. After gel polymerization, the substrates were coated with 1.5 ml of collagen I solution (0.1 mg/ml; Inamed Biomaterials) and stored overnight at 4°C. On the next day, the gels were washed with phosphate buffered saline, hydrated with 2 ml of DMEM supplemented with 0.5% FBS and stored in an incubator at 37°C and 5% CO_2.

3. Results and Discussion

Some recent results obtained by the aforementioned optical-based techniques of the cell response to transient stretch in terms of stiffness, traction force, and F-actin dynamics are given as follows. In order to compare results from various experiments, we divided all results of each experiment by the baseline value that was measured immediately before the stretch−unstretch maneuver, and denoted the ratio as normalized results. With regards to cell stiffness, the normalized stiffness (G'n) denotes cell stiffness after transient stretch-unstretch relative to stiffness of the same cells immediately before stretch. In doing so, each cell becomes its own control, which greatly increased the statistical power.

When cells were not subjected to stretch, the cell stiffness was relatively constant. However, when a single transient stretch was applied to the cells, the normalized cell stiffness, G'n, promptly decreased immediately after the cessation of stretch, but then gradually recovered to its baseline level in about 5 min (Fig. 5). The stretch induced about 50% reduction of cell stiffness ($p < 0.01$). What may be more important is that, this physical response appeared to be independent of cell mechanotransduction signals. For example, when cells were treated with a variety of pharmacological agents that are known to inhibit cell mechanotransduction during a stretch and hold maneuver, including LY294002 (inhibits the PI3K), Triciribine (specifically inhibits the Akt/PKB), SB203580 (inhibits p38 MAP kinase pathway),[9−11] the response of cell stiffness to transient stretch hardly changed fashion, indicating that the effects of these inhibitors were negligible on cell stiffness during a transient stretch−unstretch maneuver ($p \gg 0.05$) (Fig. 5).

Furthermore, unlike the transient stretch, when cells were subjected to a similar magnitude transient compression, by an unstretch−restretch maneuver using the same punch indenter, the normalized cell stiffness, G'n, did not change as shown in Fig. 6. The different effects to cell stiffness between tension and compression can be explained by the mechanical property of cytoskeleton. In the cytoskeletal network, the actin filaments are under tension whereas the microtubules are under compression, and the contribution of microtubules to overall cell stiffness is relatively smaller. Therefore, when we apply a transient compression of moderate magnitude to cells, the microtubules bear the compression and the F-actin is not so influenced.

In accordance to the cell stiffness changes, the cell traction force microscopy results showed that the cell exhibited a similar response to a transient stretch. Immediately after the stretch−unstretch maneuver, the traction force map indicated a great extent of decrease of the overall contractile moment

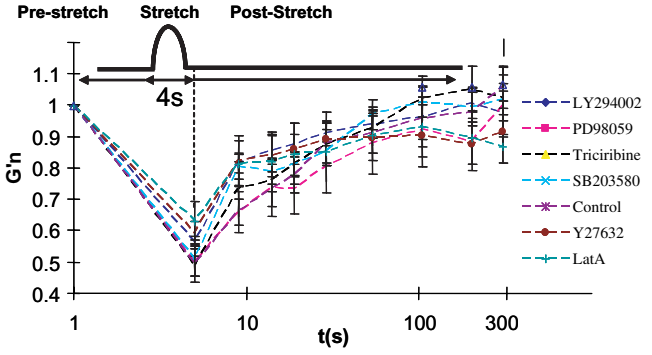

Fig. 5. Cell stiffness changes in response to a transient stretch. All results are presented as median ±SE, $n = 244-709$ beads were measured in each experiment, and Kruskal−Wallis one-way analysis was used to assess the results from different experiments, and $^{*}p < 0.05$ is considered significant — modified from our previously published results.[6]

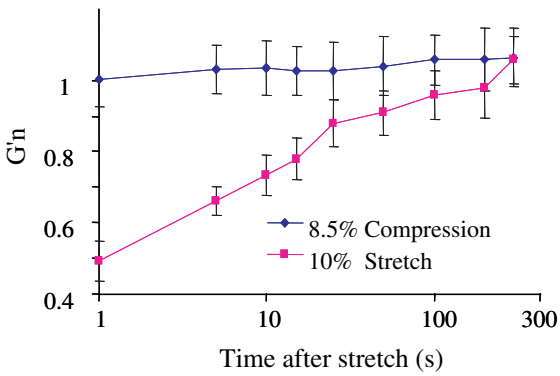

Fig. 6. Cell stiffness changes in response to either a transient stretch or a transient compression with similar magnitude of strain.

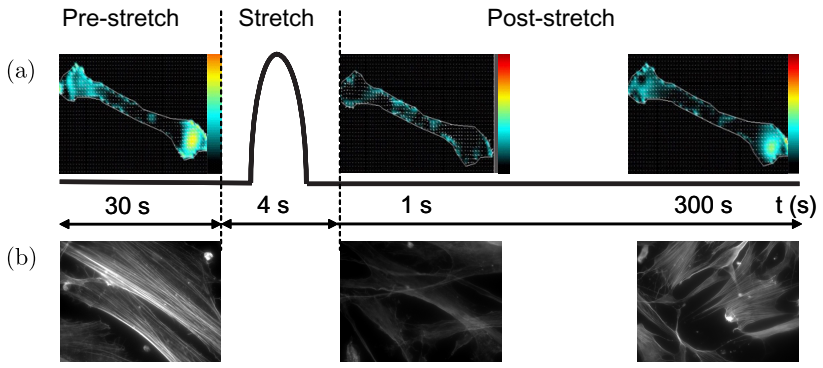

Fig. 7. Images of cell traction force microscopy (a) and F-actin filaments (b). For assessing F-actin filaments, cells cultured on polyacrylamide gel were first fixed with 4% formaldehyde in PBS (10 min) and permeabilized with 0.1% triton X-100 in PBS (10 min). Then the cells were stained with Oregon Green 488 phalloidin (Molecular Probes). Thus F-actin filaments in the cells were visualized and imaged by confocal laser scanning microscopy (Nikon Eclipse TE300, 40 × oil).

of the cell, but this reduction was largely recovered in about 5 min after the cessation of the stretch (Fig. 7, upper panel). The change of the overall contractile moment was accompanied by change in the F-actin cytoskeleton as shown by the lower panel of Fig. 7. Compared to F-actin filaments in unstretched cells within the same dish but outside the stretched region (Fig. 7, lower left image), the F-actin cytoskeleton appeared to be largely ablated immediately after exposure to the transient stretch (Fig. 7, lower middle image), and the ablation was also largely recovered in about 5 min (Fig. 7 lower right image). These results display a clear evidence of disruption of F-actin filaments immediately following stretch, and reassembly over time after stretch.

Quantitative analysis of both traction force map and fluorescent image of F-actin cytoskeleton corroborated the above observation of changes in cell traction and cytoskeleton structure. The intensity of fluorescent stained F-actin filaments was quantified by image analysis using the MetaVue software (Universal Imaging Corporation). Compared to the cells before stretch, the overall contractile moment of the cells decreased to a level of 10% relative to that of the pre-stretch but recovered to about 60% of the pre-stretch level (Fig. 8, solid bars). Similarly, the fluorescence intensity of F-actin cytoskeleton decreased by about 50% of that of pre-stretch, and almost completely recovered in 5 min (Fig. 8 empty bars). The contractile moment of F-actin intensity recovered in similar fashion after the cessation of stretch−unstretch maneuver, but with different extent of recovery. In 5 min after the cessation of the transient stretch, both cell stiffness and F-actin cytoskeleton recovered almost completely (90% and 100%, respectively), but the contractile moment only recovered up to 60%.

This difference of traction force recovery from that of cell stiffness or F-actin cytoskeleton is likely attributable to slight differences in experimental protocols because tractions were measured in single isolated cells, whereas cell stiffness and F-actin cytoskeleton measurements were performed in confluent cell layers. To further confirm these effects, the levels of filamentous (F) and globular (G) actin in cells were measured by Western blotting. When cells were subjected to transient stretch; over the short duration of the experimental maneuver, the total amount of actin must be conserved, and the relative levels of F-actin and G-actin would reflect the dynamics of shift balance of actin polymerization/depolymerization. We found that the

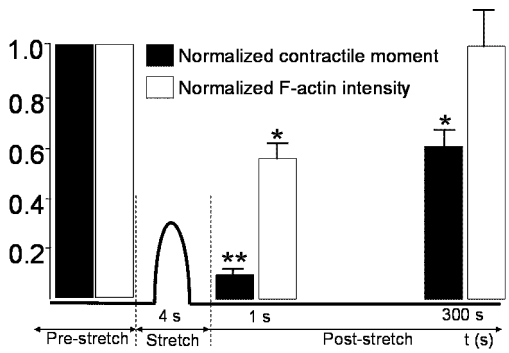

Fig. 8. The quantitative results of normalized contractile moment and F-actin intensity before and after a transient stretch−unstretch maneuver. The results are presented as median $\pm E$, $n = 9$ cells used for cell traction force microscopy, and $n = 14-29$ cells used for assessing F-actin intensity. Two-tailed unpaired Student's t-test was used for comparing group differences *, ** denote $p < 0.05$, 0.01, respectively.

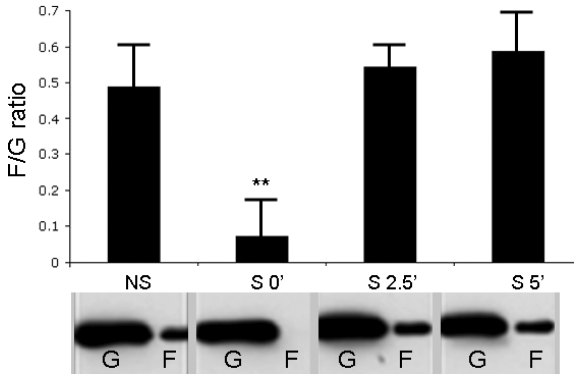

Fig. 9. The quantitative results of the ratio between filamentous (F) actin and globular (G) actin expressions before and after a transient stretch−unstretch maneuver. The results are given as mean ±SE, $n = 3$, two-tailed unpaired Student's t-test was used for comparing group difference, and ** denotes $p < 0.01$.

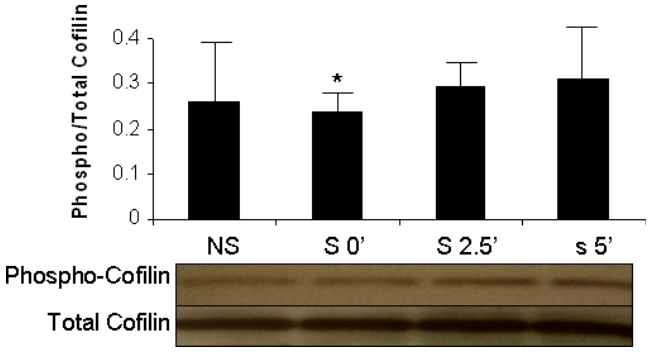

Fig. 10. The quantitative results of the ratio between phosphor-cofilin and total cofilin expressions before and after a transient stretch−unstretch maneuver. The results are given as mean ±SE, $n = 3$, two-tailed unpaired Student's t-test was used for comparing group difference, and * denotes $p < 0.05$.

profile of phosphotyrosine protein phosphorylation did not change appreciably, but there was a complete ablation of F-actin levels immediately after stretch ($p < 0.01$) and slow recovery to pre-stretch levels in 5 min (Fig. 9).

The Western blotting results of changing balance between F- and G-actin expressions confirmed that the transient stretch does cause a prompt disruption of the F-actin cytoskeleton, which in turn is largely responsible for the fluidization of the cell immediately after a transient stretch. However, it is not known what underlying mechanisms are involved in the regulation of this rapid change of actin polymerization dynamics. One possibility is that the quick loading of large strain on the F-actin filaments due to transient stretch may affect the conformation or activity of actin binding proteins such as cofilin, and leads to depolymerization of actin filaments. To test this possibility, we examined the expression level of phosphorylated cofilin in the cell before and after the transient stretch. The results indicate that the level of phosphor−cofilin indeed decreased significantly immediately after the stretch ($p < 0.05$), but quickly recovered afterward (Fig. 10). This suggests that the transient stretch caused down-regulation of cofilin activity, which is likely to contribute to the depolymerization of actin filaments. However, the decrease of phosphor−cofilin level was relatively small and may not be sufficient to fully explain the stretch-induced disruption of actin filaments. Other players and their roles in orchestrating cell fluidization/resolidification remain to be elucidated.

4. Conclusion

Taking together, these findings observed by the optically-based methods reveal that for the adherent cell such as the isolated HBSM cell, a transient stretch induces quick disruption of the F-actin cytoskeleton in the cell, followed by slow reassembly. This F-actin cytoskeleton dynamic change appears to underlie the prompt ablation and slow recovery of both cell stiffness and contractile moment ablation. These phenomena induced by transient stretch is either different from those induced by steady stretch or absent when a transient compression is applied to the cell. This implies that, the adherent cell as a mechanosensor can detect and properly respond not only to the magnitude (the amount), but also the direction and fashion (the way) of mechanical loadings.

References

1. B. Fabry, G. N. Maksym, S. A. Shore, P. E. Moore, R. A. Panettiery, J. P. Butler, J. J. Fredberg, "Selected contribution: Time course and heterogeneity of contractile responses in cultured human airway smooth muscle cells," *J. Appl. Physiol.* **91**, 986−994 (2001).
2. M. Dembo, Y. L. Wang, "Stresses at the cell-to-substrate interface during locomotion of fibroblasts," *Biophys. J.* **76**(4), 2307−2316 (1999).
3. N. Wang, I. M. Tolic-Norrelykke, J. Chen, S. M. Mijailovich, J. P. Butler, J. J. Fredberg, D. Stamenovic, "Cell prestress. I. Stiffness and prestress are closely associated in adherent contractile cells," *Am. J. Physiol. Cell Physiol.* **282**(3), C606−C616 (2002).

4. X. Trepat, L. H. Deng, S. S. An, D. Navajas, D. J. Tschumperlin, W. T. Gerthoffer, J. P. Butler, J. J. Fredberg, "Universal physical responses to stretch in the living cell," *Nature* **447**(7144), 592−596 (2007).
5. R. Krishnan, C. Y. Park, Y.-C. Lin, J. Mead, R. T. Jaspers, *et al.*, "Reinforcement versus fluidization in cytoskeletal mechanoresponsiveness," *PLoS ONE* **4**(5), e5486 (2009). doi:10.1371/journal.pone.0005486.
6. C. Chen, R. Krishnan, E. Zhou, A. Ramachandran, D. Tambe, *et al.*, "Fluidization and resolidification of the human bladder smooth muscle cell in response to transient stretch," *PLoS ONE* **5**(8), e12035 (2010). doi:10.1371/journal.pone.0012035.
7. J. P. Butler, I. M. Tolic-Norrelykke, B. Fabry, J. J. Fredberg, "Traction fields, moments, and strain energy that cells exert on their surroundings," *Am. J. Physiol. Cell Physiol.* **282**(3), C595−C605 (2002).
8. I. M. Tolic-Norrelykke, J. P. Butler, J. Chen, N. Wang, "Spatial and temporal traction response in human airway smooth muscle cells," *Am. J. Physiol. Cell Physiol.* **283**(4), C1254−C1266 (2002).
9. R. M. Adam, "Recent insights into the cell biology of bladder smooth muscle," *Nephron. Exp. Nephrol.* **102**, e1−e7 (2006).
10. R. M. Adam, S. H. Eaton, C. Estrada, A. Nimgaonkar, S. C. Shih, *et al.*, "Mechanical stretch is a highly selective regulator of gene expression in human bladder smooth muscle cells," *Physiol. Genomics* **20**, 36−44 (2004).
11. R. M. Adam, J. A. Roth, H. L. Cheng, D. C. Rice, J. Khoury, *et al.*, "Signaling through PI3K/Akt mediates stretch and PDGF-BB-dependent DNA synthesis in bladder smooth muscle cells," *J. Urol.* **169**, 2388−2393 (2003).